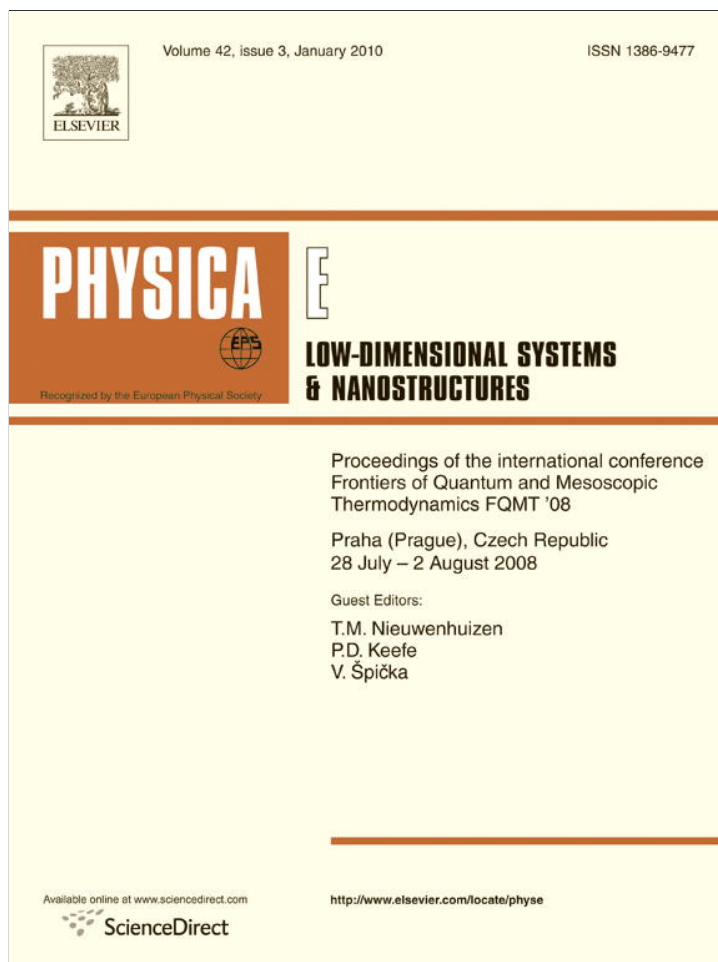


Provided for non-commercial research and education use.
Not for reproduction, distribution or commercial use.



This article appeared in a journal published by Elsevier. The attached copy is furnished to the author for internal non-commercial research and education use, including for instruction at the authors institution and sharing with colleagues.

Other uses, including reproduction and distribution, or selling or licensing copies, or posting to personal, institutional or third party websites are prohibited.

In most cases authors are permitted to post their version of the article (e.g. in Word or Tex form) to their personal website or institutional repository. Authors requiring further information regarding Elsevier's archiving and manuscript policies are encouraged to visit:

<http://www.elsevier.com/copyright>



Semiclassical formulation of non-Markovian quantum Brownian motion

Werner Koch^a, Frank Großmann^a, Joachim Ankerhold^{b,*}, Jürgen T. Stockburger^b

^a Institut für Theoretische Physik, Technische Universität Dresden, D-01062 Dresden, Germany

^b Institut für Theoretische Physik, Universität Ulm, D-89069 Ulm, Germany

ARTICLE INFO

Available online 24 June 2009

Keywords:

Dissipative quantum systems
Stochastic Schrödinger equation
Semiclassical approximation
Non-Markovian dynamics

ABSTRACT

Recently it was shown [W. Koch, F. Grossmann, J.T. Stockburger, J. Ankerhold, Phys. Rev. Lett. 100 (2008) 230402] that a combination of an exact stochastic decomposition of non-Markovian dissipative quantum dynamics with the time-dependent semiclassical initial value formalism offers a powerful tool to describe quantum Brownian motion in domains of parameter space where other approaches fail. In particular, low temperatures, stronger friction, a wide range of spectral bath densities, and continuous nonlinear systems can be treated. Details of this formulation including its numerical implementation and the impact of non-Markovian phenomena are discussed for the exactly solvable case of a harmonic oscillator.

© 2009 Elsevier B.V. All rights reserved.

1. Introduction

Brownian motion, that is the fate of a heavy particle immersed in a fluid of lighter particles, is the prototype of a dissipative system coupled to a thermal bath. The corresponding classical theory is well-established and formulated in terms of generalized Langevin equations for stochastic trajectories or Fokker–Planck equations for phase-space densities. Within this framework weak and strong friction as well as processes in presence of colored noise have been studied. In contrast, for a long time the quantum mechanical theory could handle only a weak interaction between “system” and “bath” so that master equations for the reduced density matrix have been derived perturbatively. This type of approach has been followed very successfully, e.g. in quantum optics [1].

Based on the work by Feynman and Vernon [2] it has been shown in the 1980s how to take advantage of the path integral representation to gain a formally exact expression for the reduced density as a sum of forward and backward paths, which is valid for arbitrary damping strength and temperature [3]. These two sets of paths arise from the two time evolution operators in the expression for the full density of the total compound, i.e., $W(t) = \exp(-iHt/\hbar)W(0)\exp(iHt/\hbar)$, where H is the total Hamiltonian. In the reduced description the influence of the bath emerges as time-nonlocal kernels including also a coupling between forward and backward paths. This feature, which is characteristic for quantum theory, makes a direct evaluation of the path integral impossible apart from the case of quadratic systems (harmonic oscillator). Another consequence of

the non-Markovian nature of quantum Brownian motion is that in general there exists no “simple” (i.e. tractable) equation of motion for the density.

Everything becomes simpler in the domains of weak and strong dissipation, where, as mentioned above, master equations have been in use in the former one and the quantum-Smoluchowski equation in the latter one [4]. In both cases though, non-Markovian effects disappear due to a sort of coarse graining in time. The central question thus arises: Is there any efficient methodology to attack the formally exact expression for the density matrix directly? Progress in this direction has been made in two ways. First, numerical schemes like Quantum Monte Carlo approaches have been shown to work for systems with a discrete Hilbert space (tight-binding) [5]; second, it was shown that the path integral dynamics can be mapped exactly onto a stochastic Liouville–von Neumann equation with complex noise forces [6]. Equivalently, a system of two Schrödinger equations coupled by two complex noise forces can be formulated. Unfortunately, a direct numerical calculation of these stochastic Schrödinger equations is plagued by severe convergence problems [7].

There is thus need for a formulation of quantum Brownian motion which can be employed efficiently, treats the system–bath interaction exactly, and preserves the quantum nature of the bare bath. In fact, such a formulation has been developed recently in Ref. [8]. The basic idea is to apply an extremely accurate and powerful semiclassical representation of the quantum propagator in terms of phase-space coherent states [9] to solve the stochastic Schrödinger equations. In the absence of a bath this approach captures interferences and coherences and, as a leading term in an asymptotic series [10], can be extended to describe also deep quantum tunneling [11]. This way, quantum Brownian motion appears for each realization of the complex noise forces as a randomly driven system dynamics obtained from stochastic

* Corresponding author.

E-mail address: joachim.ankerhold@uniulm.de (J. Ankerhold).

orbits. Upon averaging over the noise distributions the full density matrix is recovered. From a semiclassical point of view this method is a type of uniform approximation and thus free of caustics. From the point of view of dissipative quantum dynamics this semiclassical Brownian motion (SCBM) approach starts from an approximation, a very accurate though, of the bare system and treats the bath and its interaction exactly. It is thus able to describe non-Markovian phenomena, stronger friction, very low temperatures, and a wide class of spectral bath densities. While the practicability of the SCBM has been demonstrated in Ref. [8], in this paper we give a more detailed account on its numerical implementation and non-Markovian effects by analysing the case of a damped harmonic oscillator. For this model exact analytical results are known and the SCBM is numerically exact as well.

In Section 2 we briefly recall the central results of the Feynman–Vernon theory and the mapping onto stochastic Schrödinger equations. The semiclassical propagator is introduced in Section 3. Details about the numerical implementation are described in Section 4. To discuss the impact of non-Markovian effects, Section 6, the well-known Markovian Caldeira–Leggett master equation is specified in Section 5.

2. Unraveling of the Feynman Vernon influence functional

We start with the standard decomposition of the total Hamiltonian

$$\hat{H} = \hat{H}_S + \hat{H}_B + \hat{H}_I \quad (1)$$

as a sum of a system part, that for reasons of simplicity shall in the sequel depend on one degree of freedom x only, a bath part consisting of an infinity of harmonic oscillators together with a bilinear interaction between them. In case of a factorized initial density with a bath residing in thermal equilibrium at temperature T one derives a path integral expression for the time-evolution of the reduced density matrix of the form [3]

$$\rho(x_f, x'_f, t) = \int dx_i dx'_i \rho(x_i, x'_i, 0) \int D[x_1] D[x_2] \times \exp\left\{\frac{i}{\hbar} (S_S[x_1] - S_S[x_2])\right\} F[x_1, x_2], \quad (2)$$

where the two real time paths x_1 and x_2 run in time t from x_i and x'_i to x_f and x'_f , respectively. They are coupled by the influence functional, which takes the form $F[y, r] = \exp(-\Phi[y, r]/\hbar)$ with

$$\Phi[y, r] = \frac{1}{\hbar} \int_0^t du \int_0^u dv y(u) [L'(u-v)y(v) + 2iL''(u-v)r(v)] + i\mu \int_0^t du y(u)r(u), \quad (3)$$

where $y = x_1 - x_2$, $r = (x_1 + x_2)/2$ denote difference and sum paths, respectively. The complex valued friction kernel $L(t) = L'(t) + iL''(t)$ is related to the force–force auto-correlation function of the bath and completely determined by its spectral density $J(\omega)$ and inverse temperature β . The static susceptibility denoted by $\mu = -\int_0^\infty du L''(u)/(2\hbar)$ is a property of the reservoir.

The above formula is an exact expression for the reduced density matrix. It has been the starting point for further analytical treatments as well as numerical evaluations via path integral Monte Carlo techniques [5]. With respect to the former ones perturbative approaches for weak and strong friction, respectively, have been put forward leading for weak dissipation/high temperature particularly to the Caldeira–Leggett master equation discussed below. An exact re-formulation based on a stochastic unraveling of forward and the backward paths has been achieved

in Ref. [6]. This procedure leads to

$$\rho(x_f, x'_f, t) = \int dx_i \int dx'_i \rho(x_i, x'_i, 0) \times M[K_{z_1}(x_f, t; x_i, 0)(K_{z_2}(x'_f, t; x'_i, 0))^*], \quad (4)$$

where M denotes the average over noise realizations z_j ($j = 1, 2$), with the noise augmenting the system actions via

$$S_{z_j}[x_j] = S_S[x_j] + \mu \int_0^t du x_j(u)^2 + \int_0^t du x_j(u) z_j(u) \quad (5)$$

in the path integral expressions of the respective propagators K_{z_j} . This stochastic unraveling differs from a similar one by Strunz et al. [12] through the appearance of two noise variables, allowing for the elimination of quantum memory effects.

Now, when representing a general initial density operator through $\hat{\rho}(t=0) = |\Psi_1\rangle\langle\Psi_2|$ (or through an ensemble of such projectors) one arrives at two Schrödinger equations coupled via two noise forces, i.e.,

$$i\hbar|\dot{\Psi}_1\rangle = \left[H_S - \zeta(t)x + \frac{\mu}{2}x^2 - \frac{\hbar}{2}v(t)x \right] |\Psi_1\rangle, \quad (6)$$

$$i\hbar|\dot{\Psi}_2\rangle = \left[H_S - \zeta_*(t)x + \frac{\mu}{2}x^2 + \frac{\hbar}{2}v_*(t)x \right] |\Psi_2\rangle, \quad (7)$$

where $\zeta(t) = \frac{1}{2}[z_1(t) + z_{2*}(t)]$ and $v(t) = (1/\hbar)[z_1(t) - z_{2*}(t)]$. The reduced density matrix (2) is obtained exactly by averaging $\hat{\rho}$ calculated from Eqs. (6) and (7) for individual representations of the noise when the correlations of ζ and v reproduce the integral kernel of the influence functional: $M[\zeta(t)\zeta(t')] = L'(t-t')$, $M[\zeta(t)v(t')] = (2i/\hbar)\Theta(t-t')L''(t-t')$, and $M[v(t)v(t')] = 0$ (Θ denotes the Heaviside step function).

Even though the above linear Schrödinger equations capture quantum Brownian motion in an appealing and transparent form, they are of limited use for practical calculations since individual samples do not stay normalized. This in turn slows down convergence and makes a direct sampling impractical [13,6]. One way out is to impose norm conservation for each individual noise realization. It was shown [6,7] that this condition can be implemented while keeping the formulation exact when one (i) replaces $x \rightarrow x - \bar{r}$ in the v -dependent terms in Eqs. (6) and (7) with an arbitrary “reference trajectory” $\bar{r}(t)$ and (ii) modifies the noise probability measure accordingly, which is equivalent as to putting

$$\zeta \rightarrow \tilde{\zeta} = \zeta - \int_0^t du \chi(t-u)\bar{r}_u, \quad (8)$$

with $\chi(u) = -\Theta(u)L''(u)/2\hbar$ being the response function of the reservoir. In fact, with the choice $\bar{r}_u = \langle\Psi_1|x|\Psi_2\rangle_u$, the diffusion of $\text{tr}\hat{\rho}$ is eliminated. Unfortunately, this does solve the problem only partially since this mapping can lead to subtle mathematical difficulties limiting the times for which numerical simulations are stable [7]. However, there are two situations known to be free of such instabilities, namely, linear systems and the classical limit. The idea which we followed in Ref. [8] was thus to combine the stochastic quantum dynamics with a semiclassical propagation scheme based on coherent states, the so-called Herman–Kluk (HK) representation of the quantum propagator [9].

3. Herman–Kluk semiclassical IVR

It was shown recently in Refs. [10,11] that the quantum mechanical propagator $K = \exp(-i\hbar t/\hbar)$ can exactly be represented as an asymptotic series in \hbar in terms of phase-space integrals,

e.g. in the form

$$K(x_f, t, x_i, 0) = \sum_{n=0}^{\infty} \hbar^n \int \frac{dp_i dq_i}{2\pi\hbar} \langle x | g_\gamma \rangle \langle p_t, q_t \rangle \times R_n(p_i, q_i, t) e^{iS(q_i, p_i, t)/\hbar} \langle g_\gamma(p_i, q_i) | x_i \rangle. \quad (9)$$

Here complex valued Gaussian wave packets $\langle x | g_\gamma \rangle \sim \exp\{-\gamma/2(x - q)^2 + (i/\hbar)p(x - q)\}$ of fixed width parameter γ have been introduced, centered around the initial phase-space points p_i, q_i and the time-evolved phase-space points p_t, q_t , respectively. The contribution of each path is weighted by its corresponding action $S(q_i, p_i, t)$ and the pre-exponential factors R_n are calculated recursively from R_0 , where the latter one contains a complex valued combination of stability matrix elements. When only the leading term in the above series is retained ($n = 0$), one arrives at the initial value representation for the semiclassical propagator pioneered by Herman and Kluk [9], i.e., $K(x_f, t, x_i, 0) \approx K_{\text{HK}}(x_f, t, x_i, 0)$. Already this leading order approximation has turned out to be an extremely powerful and accurate tool to capture the time evolution of even high-dimensional systems including typical quantum phenomena such as interferences and coherences. By taking into account next two order contributions ($n = 1, 2$) also processes involving deep tunneling can be described [11]. Here, we concentrate on a one-dimensional problem without barrier and thus work within the standard HK-approximation.

One now observes that the propagation of *individual samples* of the stochastic processes (6) and (7) by the HK propagator is, apart from simple potential terms of quadratic order, equivalent to the time evolution of a closed systems in presence of stochastic external forces. The action reads as in Eq. (5) with the replacement of the noise force described in Eq. (8). Obtaining the final density matrix $\rho(x_f, x_f', t)$ involves three Monte Carlo integrations, two over the forward and backward phase spaces of the semiclassical propagators and an additional one over the noise trajectory distribution. The expectation is that the asymptotic convergence properties of the HK propagator for a closed systems [14] are ‘inherited’ by our stochastic samples.

How does the semiclassical dynamics corresponding to the transformed versions of Eqs. (6) and (7) look like? Crucial is the fact that the complex forces ξ and v do not extend the phase space to complex numbers. Namely, since the frozen Gaussians are, up to a trivial phase factor, coherent states $|\alpha\rangle = e^{-|\alpha|^2/2} e^{\alpha a^\dagger} |0\rangle$ with

$$\alpha = \sqrt{\frac{\gamma}{2}} \left(q + \frac{ip}{\hbar\gamma} \right), \quad (10)$$

it is obvious that complex values of q and p lead only to states already described by a real-valued phase space. Thus, the classical equations of motion derived from (6) and (7) read ($j = 1, 2$)

$$\frac{d}{dt} \alpha_j = \sqrt{\frac{\gamma}{2}} \left(\frac{p_j}{m} - \frac{i}{\hbar\gamma} V'(q_j) + \frac{i}{\hbar\gamma} f_j \right) \quad (11)$$

with $f_1 = \xi + (\hbar/2)v$ and $f_2 = \xi^* - (\hbar/2)v^*$, to be solved for real q_j and p_j using (10). In the limit $\hbar \rightarrow 0$ and upon integrating by parts in (8), the classical Langevin equation is indeed recovered from Eq. (11).

Semiclassically, the reference trajectory is again obtained by demanding that the v -dependent terms in Eqs. (6) and (7) do not change the trace of the sample. One then finds the simple condition

$$\bar{r}_u = (\alpha_1 + \alpha_2^*) / \sqrt{2\gamma}. \quad (12)$$

This definition of \bar{r}_u includes a single pair of semiclassical trajectories so that it is suggestive to merge the integrations over the two HK phase spaces and the function space of noise trajectories $\xi(t)$ and $v(t)$ into a joint Monte Carlo sampling scheme.

4. Sampling strategy

The naive procedure to calculate the semiclassical time evolution would be to generate first phase-space trajectories for an individual noise realization until the HK-propagation is converged and only afterwards to average over a sufficiently large number of noise realizations. Thereby, the three integrations are performed via Monte Carlo sampling. However, this procedure is not only not necessary, but it is also not very efficient. In practice, all three samplings can be combined such that for each trajectory pair a separate noise sample is generated and two phase-space points for the forward and backward trajectories are chosen. For this combination the semiclassical trajectories are evaluated and the desired expectation values are computed. The results are then accumulated. Since each trajectory evaluation contributes to a different noise sample, the sample count is increased by the number required to converge the semiclassical propagator, which is typically on the order of $10^3 - 10^4$ for a one-dimensional system.

Using a single pair of semiclassical trajectories for each noise sample also greatly simplifies the computation of the guide trajectory as already mentioned above. For a harmonic system it can even be performed analytically. For $N > 1$ trajectory pairs per noise sample, either the wave function has to be computed numerically before the position expectation value can be obtained or N^2 analytical exponentials have to be computed. Fig. 1 shows a comparison of the convergence properties for such a simple harmonic test case (for details see below). The three curves were obtained for the naive sampling, the combined sampling, and for the combined sampling including a guide trajectory. Obviously, the naive sampling is far from being converged. The general trend for longer times not even closely matched, but rather the results are also severely plagued by ‘spikes’. In order to eliminate these, sample and trajectory count have to be increased tremendously. The combined sampling, however, improves convergence significantly and acceptable results can be obtained with only a moderate increase of the number of trajectory pairs. Convergence can be attained even faster by also including the guide trajectory (12). This way, as seen in Fig. 1, numerical data basically coincide with the analytical result (not shown).

For anharmonic systems the combined sampling with guiding trajectory is crucial to even approach convergence (see Ref. [8]). For these potentials the presence of complex noise forces may lead to significant imaginary components of the action. In theory these imaginary parts average to zero. In practice, however, one

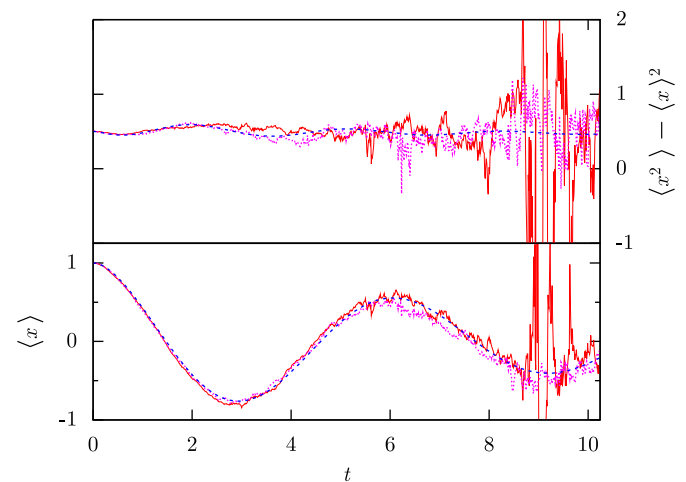


Fig. 1. Expectation value of variance and position for three different noise samplings: naive sampling (solid), improved sampling (dotted), improved sampling and guide trajectory (dashed). Parameters given in Section 6

faces a problem similar to the dynamical sign problem known from standard HK-propagations. Since the sample count is finite and imaginary parts of the action produce an exponentially large/small contribution to the integrand, a specific sample with an unusually large negative imaginary action may not be compensated for by other samples. There are a number of ways to deal with this situation. The idea to simply increase the number of samples fails, as one may expect, since it leads to a typically exponential increase in computer time. A feasible scheme would be to detect these “pathological” samples (e.g. define a limiting value for the imaginary component of the action) and to remove them before adding up. However, depending on the parameters of the calculation and the potential considered, the fraction of such samples can be larger than a few percent. Thus simply eliminating their contribution might have significant and unpredictable impact on the results.

A more subtle procedure is based on the observation that an imaginary part of the action is not just a consequence of the chosen noise sample but also depends strongly on the chosen initial phase-space coordinates. Thus, upon detecting that a certain trajectory pair is of adverse character, one can keep the corresponding noise sample and attach to it two newly generated phase-space points. Even better, one can keep both, noise sample and initial phase-space points, and interchange this set with another one corresponding to a second adverse trajectory pair. Thus, neither the statistics of the noise distribution nor the semiclassical sampling of the initial phase spaces are altered. The only effect of this procedure is the introduction of a correlation between the sampling of the phase spaces and the noise distribution. Explicit calculations with and without this swapping procedure show though that apart from the removal of “spikes” due to adverse samples, there is no systematic effect introduced on the time dependence of the physical observables.

5. Caldeira–Leggett master equation

For sufficiently elevated temperatures the exact path integral expression (2) can be represented in an approximate time evolution equation for the reduced density, the so-called Caldeira–Leggett (CL) master equation [17]. One crucial assumption is that the memory time of the environment, i.e., the correlation time of the noise forces, is small compared to the relaxation time scale. Accordingly, only Markovian properties of the bath survive. The CL-master equation is thus a convenient reference to study to what extent non-Markovian effects influence the full quantum dynamics even in ranges of parameter space beyond its strict applicability. Specifically, one has

$$i\hbar \dot{\hat{\rho}}(t) = [H_S, \hat{\rho}(t)] + \frac{\eta}{2m} [x, [p, \hat{\rho}]_+] - \frac{i\eta}{\hbar\beta} [x, [x, \hat{\rho}]] \quad (13)$$

with the classical damping constant $\eta = \lim_{\omega \rightarrow 0} J(\omega)/\omega$ [$J(\omega)$ is the spectral density of the bath]. Apparently, the quantum dynamics of the bare system is fully described, while the bath has lost its quantum nature completely so that it reacts instantaneously on the system and retardation effects are absent. Further, asymptotically (for long times) the density matrix reduces to an expression for the thermal equilibrium density whose statistics of position and momentum are valid only at higher temperatures.

6. Results and discussion

In the following we will highlight a few features of the SCBM approach by studying the one-dimensional damped harmonic

oscillator under varying environmental parameters. The reason for this is twofold: on the one hand exact analytical results for this system are available for comparison and on the other hand the HK-propagation becomes exact which allows for carefully studying convergence properties of various numerical algorithms. Specifically, the system potential is

$$V(x) = \frac{1}{2}m\omega^2 x^2,$$

where we set $m = 1$, $\omega = 1$ for convenience in the sequel. The initial wave packet will be a Gaussian shifted in coordinate space away from the minimum of the potential by $\langle x \rangle_0 = 1$ and with zero momentum. The spectral density of the bath oscillators is taken to be Ohmic with a choice of two different cutoff behaviors, namely,

$$J_\kappa(\omega) = \frac{\eta\omega}{(1 + \omega^2/\omega_c^2)^\kappa} \quad \text{with } \kappa = 1, 2, \quad (14)$$

where the dimensionless coupling strength is denoted by η and the cutoff frequency by ω_c . The form J_2 facilitates numerical computation as its narrower spectral width allows for a larger time step to be chosen whereas J_1 simplifies the comparison with analytical results as explicit evaluations of the general analytical expressions are straightforward for a Drude–Lorentz type of cutoff (see e.g. Ref. [16]). For all examples shown in the following, the cutoff frequency is chosen to be $\omega_c = 10$, sufficiently far above the system frequency. Accordingly, non-Markovian effects in the dynamics are assumed to be basically absent at higher temperatures.

Other cutoff-procedures are possible as well, of course. A necessary requirement is though that the friction kernel $L(t)$, or for the purpose of noise generation its Fourier transform, to be given in analytical form or at least to be calculated numerically with only modest computational effort. A rather practical limit is furthermore imposed by implementing the convergence improving properties of the guide trajectory. In this case, the integral in Eq. (8) needs to be evaluated at every time step.

We start by comparing various sampling strategies as already discussed in Section 4 in Fig. 1. For this purpose, the spectral density J_2 was chosen together with an inverse temperature $\beta = 2.0$ and a coupling strength $\eta = 0.2$. We emphasize that the differences in the approaches towards convergence are not due to a higher trajectory count. The data for all three graphs were obtained with about 10^6 trajectory pairs so that the improvements are sole results of a combined sampling and an inclusion of a guide trajectory.

For any realistic system the spectral density has a finite cutoff frequency. In Figs. 2–4 we also demonstrate the significance of choosing the correct type of cutoff behavior. Once again the lower panel depicts the expectation value of position and the upper ones its variance calculated within the SCBM scheme for two different numbers of trajectory pairs. For comparison the analytical expressions from Ref. [15] for a purely ohmic environment ($\omega_c \rightarrow \infty$) as well as for a Drude–Lorentz density J_1 are shown. For all cases the inverse temperature of the bath is $\beta = 0.5$ and the coupling strength is $\eta = 0.2$. While in Fig. 2 differences are hardly discernable, the detailed plots of Figs. 3 and 4 clearly reveal that the analytical results for a purely ohmic bath deviate significantly from those with a finite cutoff at early but also at intermediate times. Further, a fourfold increase of the trajectory count in the SCBM scheme (upper panel of Fig. 4) improves convergence substantially and basically reproduces the exact data.

To quantify the errors incurred by invoking a high temperature Markov approximation in the form of the Caldeira–Leggett master equation and to demonstrate the accuracy of the SCBM scheme, we compare the latter ones with analytical results and those obtained by means of a finite difference implementation in

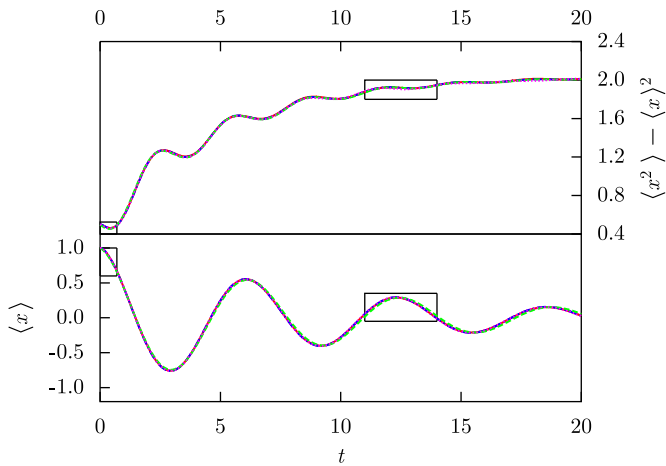


Fig. 2. Expectation values of variance and position for a harmonic oscillator gained with SCBM calculations: 4×10^6 trajectory pairs (solid), 1×10^6 trajectory pairs (dotted), and analytical results [the latter ones without cutoff (dashed) and with Drude cutoff (dash-dotted)]. Boxes indicate the ranges of the blowups in Figs. 3 and 4.

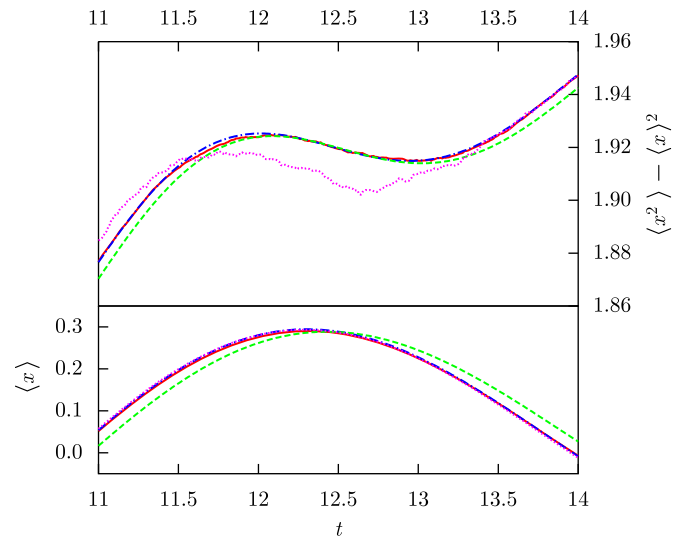


Fig. 4. Same as Fig. 2, in detail.

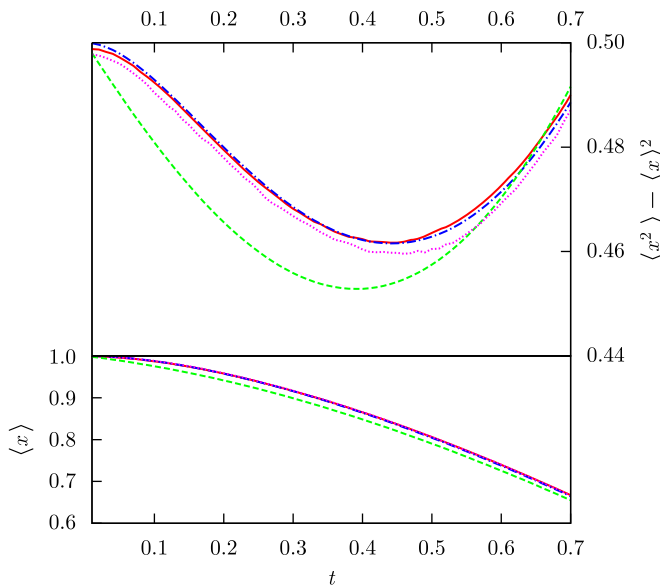


Fig. 3. Same as Fig. 2, in detail.

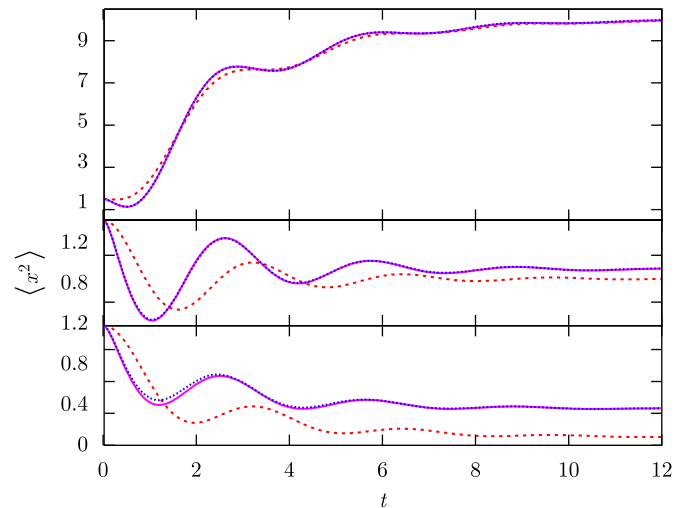


Fig. 5. Second moment of the density $\langle x^2 \rangle$: $\beta = 0.1$ (top panel), $\beta = 1$ (middle panel), and $\beta = 10$ (bottom panel). SCBM calculations (solid line), analytical results (dotted), and Caldeira–Leggett (dashed) ($\eta = 0.4$).

position space of the CL master equation (for details see Ref. [18]). For the sake of comparability with the analytical results we again select a Drude–Lorentz cutoff J_1 . In Fig. 5 the second moment of coordinate for three different temperatures and for each of the three methods is shown. Even at a relatively high temperature (upper panel, $\beta = 0.1$) the dynamics according to the CL clearly deviates from the exact data at all intermediate times. Since in this temperature range the CL provides the correct asymptotic value for the thermal equilibrium, these deviations must be attributed to the non-Markovian nature of the exact quantum dynamics. At lower temperatures also the asymptotic behavior is no longer captured and the dynamics for intermediate times scales is strongly off the exact data in amplitude and phase. The SCBM simulations provide extremely accurate results over the whole temperature range. They were obtained with 5×10^6 trajectory pairs which requires a computation time of a few hours on a desktop PC.

To summarize, we have shown that an improved SCBM scheme (combined sampling and guide trajectory) reproduces nicely the known analytical results for the harmonic oscillator in a wide

range of parameters and far beyond the applicability of the CL master equation. For anharmonic potentials analytical exact expressions are no longer available and one can assume that CL results are accurate only for narrow windows of parameters. In contrast, as already demonstrated in Ref. [8], the SCBM can be employed efficiently also in domains of parameter space where no other approximate method is known to work. It remains to be seen how substantial deviations are quantitatively. Apart from this point, the SCBM scheme provides a level of accuracy where the form of the bath spectral density matters up to high frequencies on the order of the cutoff frequency. It can thus be used as a powerful tool to sensitively probe the quantum dissipative dynamics for various models of the environment.

Acknowledgments

We acknowledge financial support by the Deutsche Forschungsgemeinschaft (W.K. and F.G., GR 1210/4-1; J.A. and J.T.S., SFB569) and by the German Israeli Foundation (J.A., G-790-113.14).

References

- [1] C.W. Gardiner, Quantum Noise, Springer, Berlin, 1991.
- [2] R.P. Feynman, F.L. Vernon, Ann. Phys. (NY) 24 (1963) 118.
- [3] U. Weiss, Quantum Dissipative Systems, World Scientific, Singapore, 2008.
- [4] J. Ankerhold, P. Pechukas, H. Grabert, Phys. Rev. Lett. 87 (2001) 086802;
J. Ankerhold, P. Pechukas, H. Grabert, Phys. Rev. Lett. 101 (2008) 119903.
- [5] See e.g.: L. Mühlbacher, J. Ankerhold, J. Chem. Phys. 122 (2005) 184715 and references therein.
- [6] J.T. Stockburger, H. Grabert, Phys. Rev. Lett. 88 (2002) 170407.
- [7] J.T. Stockburger, Chem. Phys. 296 (2004) 159.
- [8] W. Koch, F. Grossmann, J.T. Stockburger, J. Ankerhold, Phys. Rev. Lett. 100 (2008) 230402.
- [9] M.F. Herman, E. Kluk, Chem. Phys. 91 (1984) 27.
- [10] S. Zhang, E. Pollak, Phys. Rev. Lett. 91 (2003) 190201.
- [11] G. Hochman, K.G. Kay, J. Phys. A 41 (2008) 385303.
- [12] W.T. Strunz, L. Diósi, N. Gisin, Phys. Rev. Lett. 82 (1999) 1801.
- [13] H.-P. Breuer, F. Petruccione, The Theory of Open Quantum Systems, Oxford University Press, Oxford, 2002.
- [14] E. Martín-Fierro, J.M. Gomez Llorente, Chem. Phys. 322 (2006) 13;
K. Kay, Chem. Phys. 322 (2006).
- [15] H. Grabert, P. Schramm, G.-L. Ingold, Phys. Rep. 168 (1988) 115.
- [16] R. Karrlein, H. Grabert, Phys. Rev. E 55 (1997) 153.
- [17] A.O. Caldeira, A.J. Leggett, Physica A 121 (1983) 587.
- [18] F. Grossmann, W. Koch, J. Chem. Phys. 130 (2009) 034105.